



An Investigation of the Interlayer Adhesion Strength in Deeper Layers of the Pavement Structure

Naphtal NTIRENGANYA*

Department of Civil Engineering
Integrated Polytechnic Regional Centre Kigali,
Rwanda

Denis KALUMBA

Department of Civil Engineering
University of Cape Town, RSA

Marius De Wet

Department of Civil Engineering
Stellenbosch University, RSA

Abstract— A road pavement structure is typically composed of different layers arranged one on top of the other, all supported by a natural or improved subgrade. The main purpose of this configuration is to provide the most effective structure with adequate potential to spread traffic loading from the surface to the subgrade with minimum damage. In spite of material properties and construction techniques, researchers have shown that the overall pavement performance is significantly influenced by the interlayer adhesion condition throughout the pavement structure ([8], [11], [21], [22]). Lack of intimate contact between layers results in them acting as individuals rather than as a thick bonded unit. This therefore induces overloading of layers which leads to premature deterioration of the entire structure due to traffic induced distresses. This work, therefore investigated the interlayer adhesion characteristics between the granular base and the lightly cemented subbase of a typical South African pavement structure. The influence of bonding condition on the overall pavement performance was also studied. A series of interlayer direct shear tests was run on 300 x 300 mm samples made of two layers: a 100mm G2 Granular Base (GB) compacted on top of the 100mm Cement Treated Subbase (CTSB) composed of a G5 material stabilised with 1.8% of cement. Effects of the CTSB scarification, normal pressure and moisture conditions were analysed whereby the results of the interlayer strength tests were compared with those of intra-layer strength tests. The comparative analysis showed that scarifying the CTSB before laying the GB enhances intimate contact between two layers and stimulates the unison interaction which, according to structural modelling results, improves the overall pavement performance.

Keywords— Interlayer adhesion, Direct shear test, Cement treated subbase, Granular base, Pavement life.

I. INTRODUCTION AND BACKGROUND

The multi-layered structure adopted as a typical South African pavement structure dates back to the Roman era. This structure was made of a large stone foundation with a surfacing course of smaller stones and gravel, confined between raised stone kerbs. The modern structure is not far from that and it comprises a surfacing layer made of asphaltic materials or concrete, base and subbase courses which might be natural or stabilised, selected layers and natural subgrade. Basically, road pavement performance is governed by the strength and stiffness of the materials available in each individual layer. The failure mechanism of main pavement materials has been well documented from many years ago and fairly well understood by pavement engineers ([9], [17], [6], [18] and [10]). In most cases, structural failure is generally linked to lack of maintenance and pavement overloading. However, the lack of mutual interaction between layers has also been identified to influence the pavement response against traffic induced stress and strain across the entire structure, and consequently affects the pavement performance.

Researchers like Kruntcheva in [11] used theoretical analysis to establish the impact of interlayer adhesion on stress-strain distribution throughout the pavement structure. They analysed a pavement structure using a multi-layered linear elastic program by considering various degrees of interface adhesion between pavement layers. The results indicated that the condition of interlayer adhesion can reduce the life of a pavement structure by up to 80%. They also conducted static linear and nonlinear two-dimensional finite element analyses and similar results were found. After realizing the influence of the interface condition on the pavement performance, different laboratory and in situ testing methods have been developed in different countries to assess the degree of adhesion between pavement layers. Since the interface was admitted to fail by shear, most of the testing approaches were typically based around shear testing. From the comparative study conducted by Raab as illustrated in [14], the direct shear test was selected as the most reliable and effective method for testing interlayer adhesion strength in the pavement structure.

Since two distinct setups of shear testing are available (i.e. devices with or without normal load), the apparatus allowing testing with the application of normal pressure has been recommended for testing granular materials. The shear testing with normal pressure was selected because it considers the dilatancy effect which is common in granular materials. The Mechanistic Design Method is one of the most popular structural design approaches used in South Africa and all over the world. The method is based on computation of stress and strain distribution in pavement layers. Most of the computation approaches used assume full friction between layers. However, researchers have shown that this assumption is not realistic and results in over-estimation of the pavement life ([11], [16], [22] and [23]). This therefore provided a solid basis to conduct this study so as to establish the interlayer bonding characteristics in road pavements.

II. RESEARCH MATERIALS AND METHODOLOGY

A. Research Materials

Two types of granular materials were used for this study: crushed hornfels stone G2 for the GB layer and blended G5 stabilised with 1.8% cement for the CTSB layer. The material selection was based on recommended specifications for the base and subbase materials of a typical South African pavement structure ([15], [20]). Research materials were collected from Lafarge quarry located in Tygerberg valley in the Western Cape, South Africa. Since the laboratory investigation was set to reflect the routine road construction practice in the field, the research materials were required to be characterized according to the South African road construction materials guidelines. Therefore various characterization tests were run with respect to South African Pavement Engineering Manual (SAPEM) and Technical Recommendations for Highways (TRH) 14 requirements. Those tests included Grading, Atterberg Limits, Apparent Relative Density (ARD), Bulk Relative Density (BRD) Modified American Association of State Highway and Transportation Officials (Mod AASHTO) compaction, California Bearing Ratio (CBR), Flakiness Index (FI), Aggregate Crushing Value (ACV), 10% Fines Aggregate Crushing Test (10% FACT), Unconfined Compressive Strength (UCS) and Indirect Tensile Strength (ITS). Results are presented in Table I. In order to ensure consistency and accurate blending of materials during specimen preparation, air-dried G2 and G5 materials were separated and stored into different fractions, by means of sieving. The G2 and G5 materials were sieved into thirteen and seven fractions, respectively and a new blending was designed for G2 materials according to TRH 14 and SAPEM requirements.

Figure 1 illustrates grading curves for the G2 and G5 materials with 19 mm maximum aggregate size.

TABLE I: AGGREGATE PHYSICAL PROPERTIES

TEST	G2	G5/CEMENT TREATED MATERIAL (CTM)
Grading	Within the envelope	Grading Modulus (GM)=2.4
Atterberg Limits	Material not plastic, Linear Shrinkage (LS) = 0.3%	Material not plastic, LS = 0.5%
ARD, BRD and Water Absorption (WA)	ARD = 2.734; BRD = 2.524; WA = 0.0%	ARD = 2.328; BRD = 2.705; WA = 0.1%
Mod AASHTO	Maximum Dry Density (MDD) = 2332kg/m ³ ; Optimum Moisture Content (OMC)= 5.4%	MDD (G5) = 2349kg/m ³ ; MDD (CTM) = 2301 kg/m ³ ; OMC =5.2%(G5&CTM)
Soaked CBR	Not Applicable	CBR at 95% Mod AASHTO = 65%; Swell at 100% = 0.0%
Flakiness Index (FI)	FI for -19;+13.2 = 13.6%; FI for -26.5;+19 = 16.5%	Not Required
ACV and 10%FACT (Wet & Dry)	ACV : Dry = 9.6%, Wet = 8.8% 10%FACT: Dry= 454kN, Wet = 415kN; ACV Ratio (wet/dry) = 91%	Not Required
UCS	Not Applicable	UCS = 6.7MPa (CTM)
ITS	Not Applicable	ITS = 320kPa

B. RESEARCH METHODOLOGY

300 mm x 300 mm x 200 mm (thickness) laboratory prepared samples were used to investigate the interlayer shear strength between the GB and the CTSB. The typical specimen was made of two different layers; the GB compacted on top of the CTSB. Both layers were compacted to 100% Mod AASHTO. To achieve the required density, the material blend was prepared according to the target MDD and volume of the layer. The automated Geocomp Shear Trac-III direct shear machine was used in this study. Apart from being fully automatic, the Shear Trac III has an advantage of allowing testing of samples with big particle sizes due to the big size of the shear box (i.e. 300 mm x 300 mm cross section).

1) *Mix Design, Compaction and Curing of the CTSB layer: The CTSB was made of G5 granular material, stabilised by 1.8% of cement. The amount of materials required to make a layer was calculated based on the target MDD obtained from the Mod AASHTO test and the volume of the layer. To ensure accuracy and uniformity, various fractions of G5 materials were weighed off and blended accordingly. Since the laboratory investigation was supposed to simulate the*

field conditions, the sample preparation procedure was developed whereby a CTSB was compacted in a steel mould using a high frequency vibratory compactor shown in Figure 2. To achieve uniform compaction, the entire CTSB layer of 100 mm thick was compacted into two sub-layers. During the compaction exercise, the complete interlock between two sub-layers was achieved by scarifying the top surface of the first completed sub-layer before casting the second one. After the compaction of the layer, the surface was scarified or left quasi-smooth according to the experimental design requirements. Scarification was done using manual scarifying tool and electric drill.

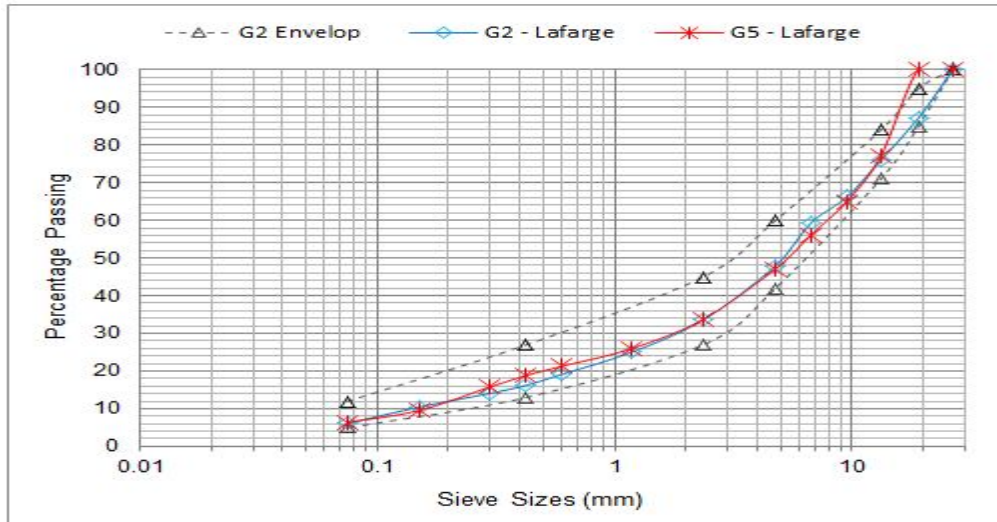


Figure 1: Grading of G2 and G5 materials

The required strength of the cement stabilized material is achieved through hydration processes which involve the combination of water, soil and cement. Practically, this is accomplished through the curing process which requires keeping the material wet after compaction for at least seven days as it is recommended by TRH 13. In this study, the curing practice involved keeping the CTSB specimen under a wet blanket and spray water for four days prior to laying the GB materials. Figure 3 shows the specimens during the curing process. This simulated what is normally done in the field whereby, after compaction of the CTSB layer, it is kept damp for up to seven days by frequent surface watering or by covering it with another pavement layer.

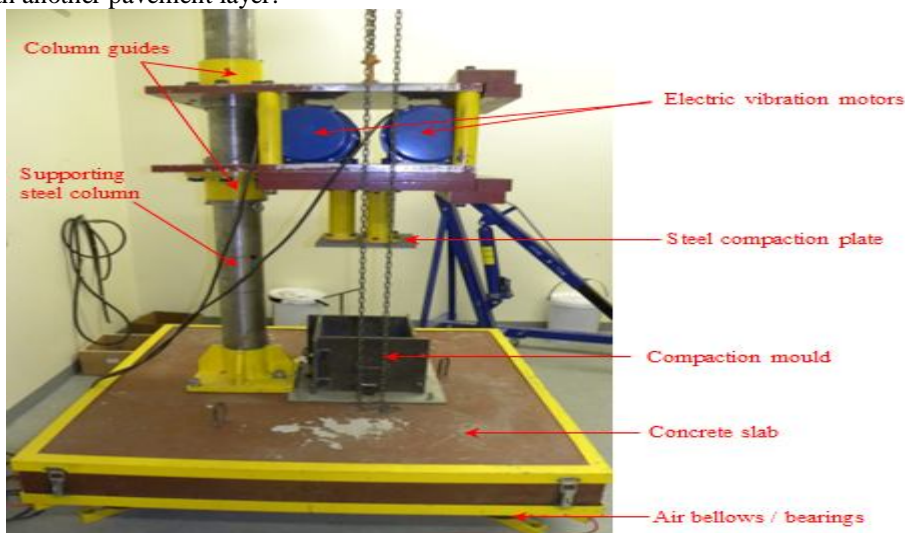


Figure 2: Vibratory compaction machine

2) *Compaction of the GB: Mixing and compaction of the G2 granular base was done in a similar way as the cemented G5 subbase. When the material was ready for compaction, four sides of the compaction mould were set around the CTSB layer and firmly fastened with bolts and nuts. To enhance specimen uniformity, the entire GB layer was compacted into two identical sub-layers with proper scarification between them as well. After compaction of the GB on top of the CTSB layer, the full specimen was taken out of the mould and carefully confined in a wooden box. Thereafter, it was kept at a temperature of 25°C for a period of three more days before testing. This was done to complete 7 days curing time of CTSB recommended by the literature and to allow homogeneous moisture distribution in the GB.*

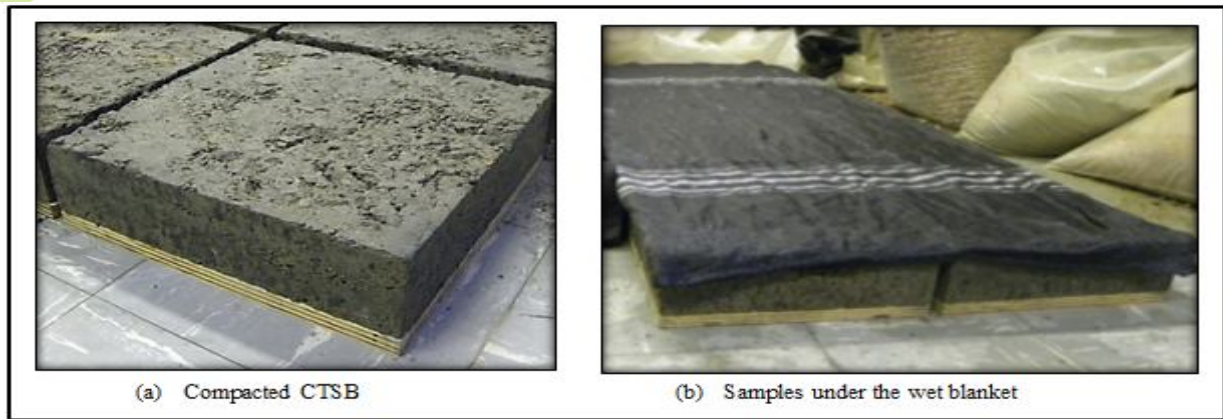


Figure 3: Illustration of main steps of the CTSB curing procedure

3) *Setting up Specimen in the Shear Box and Interlayer Shear Testing:* The automated Geocomp Shear Trac-III direct shear machine shown in Figure 4 was used for the interlayer shear testing. Even if static loading of the direct shear test does not accurately simulate horizontal dynamic loading of the pavement structure, the test was identified as the most reliable for characterization of interlayer shear strength ([14]).

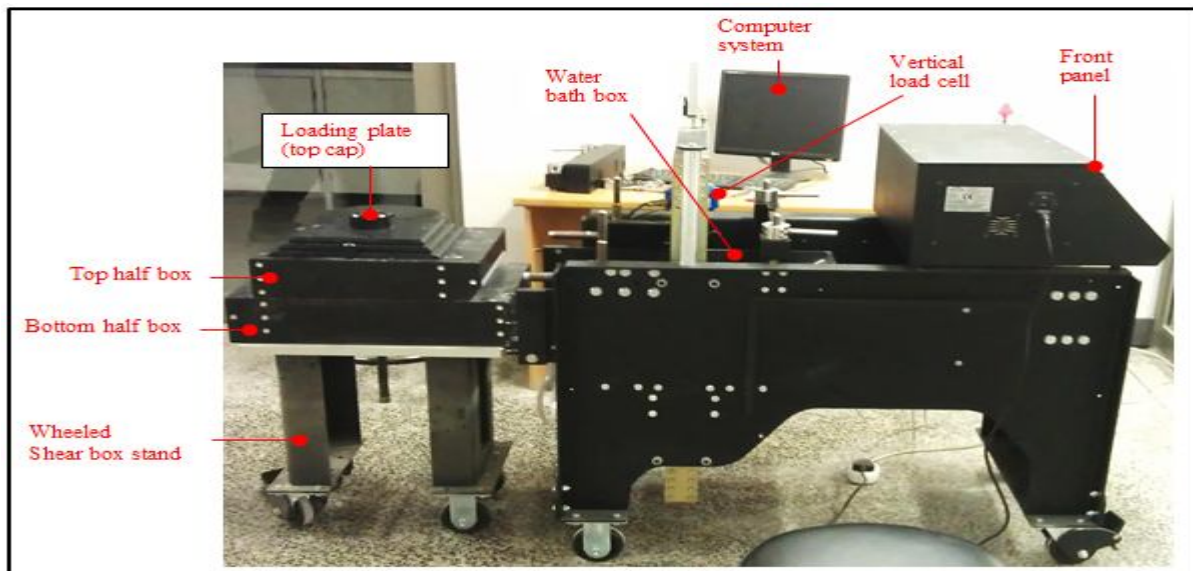


Figure 4: Photograph of Shear Trac-III

Accurate setting of the specimen into the shear testing machine was essential so as to obtain proper results. To achieve this, various trials were attempted to determine the fit-for-purpose technique which allows the sample to be placed in the shear box without disturbance. Since the shear box was made with 2 mm allowance on each side, this allowed the specimen to be lifted and slid in the box by using a pair of 500µm thick strap. When the specimen was firmly placed in the shear box, the lifting straps were removed and the shear box was properly mounted inside the Shear Trac-III housing and all set up accessories, were fixed. Extra care was devoted to the specimen preparation process and set up to accurately align the shear plane with the interface between CTSB and GB.

4) *Shear Testing Procedure:* According to the testing conditions, two types of tests were conducted: saturated and unsaturated testing. During the saturated test, the specimen was allowed to stand in water for 40 minutes before testing. 40 minutes was admitted to allow total saturation of the interlayer between CTSB and GB. Additionally, before and during the test, the water level was kept at 25 mm above the shear plane to ensure saturation consistency between the two layers. Prior to shearing the interface, a one directional consolidation phase was run to bring the specimen to the equilibrium state. Vertical displacement due to consolidation ranged between 0 and 4 mm for all tested samples. Since each specimen was adequately compacted and properly positioned in the shear box, slight movement due to consolidation pressure was localised at the top loading plate which did not affect the alignment between the shear plane and the specimen interlayer. After the consolidation phase, a gap of 5 mm was created between the two half-boxes to eliminate any possibility of metal to metal friction.

The unsaturated tests were conducted in a similar way but the sample was not soaked in water before and during test. Selection of the shear rate was based on previous studies. However, material type and sample size were also considered.

According to the research done on interlayer shear testing with the application of normal pressure, the horizontal displacement rate ranged between 1.27 and 3 mm/min ([5], [4], [2], [1] and [22]). Note that all the above listed studies involved bituminous materials and relatively small devices comparing to the Shear Trac-III system. With knowledge of the unbound behaviour of granular materials and the large size of the sample, the shear rate of 1 mm/min was decided on to provide detailed records for the unsaturated testing. For the saturated tests, the rate was reduced to 0.6 mm/min to allow for the total saturation of the interface as shearing proceeds. To achieve the research objectives, two qualitative factors and one quantitative factor influencing interlayer adhesion strength were examined. Qualitative factors included investigation of effect of CTSB surface roughness condition and material moisture condition. The quantitative factor considered the magnitude of the applied normal pressure. Each of the three factors had at least two levels of analysis. Two surface roughness conditions of the CTSB were considered: scarified and quasi-smooth, two testing moisture conditions: saturated and unsaturated, and at least two values of normal pressures (i.e. 50 and 100 kPa) for all possible combinations. Additionally, extra experimental runs were conducted to assess the effect of the maximum size of the aggregate in the CTSB whereby it was changed from 19 mm to 26 mm. This trial was limited to the scarified CTSB surface under saturated and unsaturated conditions for three applied normal pressures. In order to better understand the degree of shear resistance between GB and CTSB layers, two extreme strength conditions were selected and compared with the normal interlayer shear strength. The best condition was represented by the intra-layer shear strength whereby the shear plane was localised within one of the layers. Consequently, a set of intra-layer tests was conducted for both types of materials. Saturated and unsaturated conditions were considered and three values of normal pressure were examined. On the other hand, the worst case scenario was simulated by shearing the interface while two layers were separated by a 500 μm thick plastic sheet, placed between them. It is important to mention that at least two specimens were tested for each combination in order to eliminate any outliers.

III. RESULTS AND DISCUSSIONS

A. INTERLAYER SHEAR TESTS

Figure 5 shows the relationship between the maximum shear stress and applied normal pressure for different testing conditions of the CTSB surface before laying the GB (scarified, quasi-smooth and lined with a plastic sheet). The general observation from the results presented in Figure 5 was that the maximum shear stress increased with increased normal pressure. Moreover, it reached the highest value when the CTSB was scarified. The influence of scarification can be explained by the “saw tooth” interaction between the GB and the scarified CTSB. Scarifying the CTSB left projecting aggregates which, after the cementation process, developed strength and resistance against overturning. At the time of laying the GB layer, free aggregate particles of the layer filled up depressions in the rigid CTSB and created the so called “saw tooth” interaction. In that condition, the resistance against horizontal movement of one layer relative to another was increased by overhanging rigid aggregate particles of the CTSB which rooted deeper in the bottom layer.

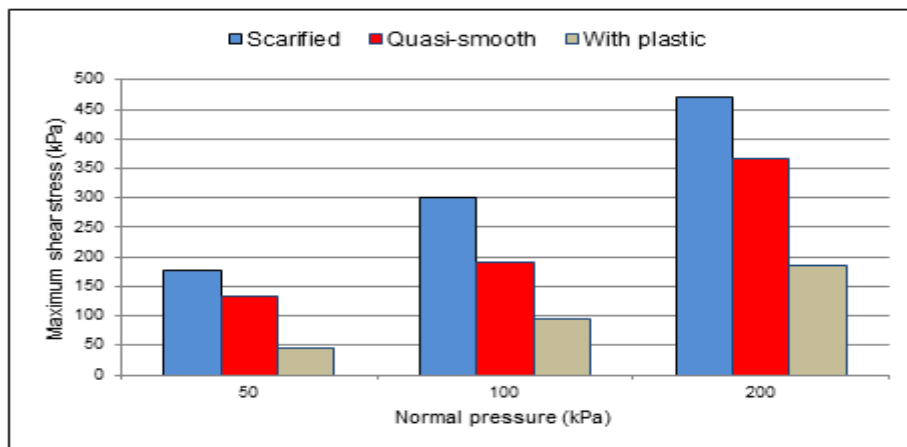


Figure 5: The typical effect of the normal pressure and CTSB surface condition on the interlayer shear stress ([25])

For each testing variable, the maximum shear stresses were deduced from the shear stress-horizontal displacement graphs and thereafter, plotted against their respective normal pressures. The best straight line fitted through three respective points corresponding to three normal pressures defined the Mohr-Coulomb failure envelope. The slope of the line defined the interlayer friction coefficient (μ) while the intercept on the vertical axis gave the interlayer cohesion (c).

In Table II, values of c and μ are shown for all testing conditions while Figure 6 and Figure 7 present curves of the relationship between the shear stress and the corresponding normal pressure for intra-layer and interlayer tests from which c and μ were deduced.

TABLE II: ACHIEVED INTERLAYER FRICTION AND COHESION

MAXIMUM AGGREGATE SIZE IN CTSB (MM)	CTSB SURFACE CONDITION	SATURATION CONDITION	$\mu = \tan \phi$	FRICTION ANGLE ϕ (°)	COHESION C (kPa)
19	SCARIFIED	UNSATURATED	1.90	62.2	90.6
		SATURATED	1.56	57.3	92.4
	QUASI-SMOOTH	UNSATURATED	1.59	57.8	45.3
		SATURATED	1.13	48.5	50.0
	WITH PLASTIC SHEET	UNSATURATED	0.93	42.9	0.7
26	SCARIFIED	UNSATURATED	2.11	64.6	55.9
		SATURATED	1.86	61.7	37.5

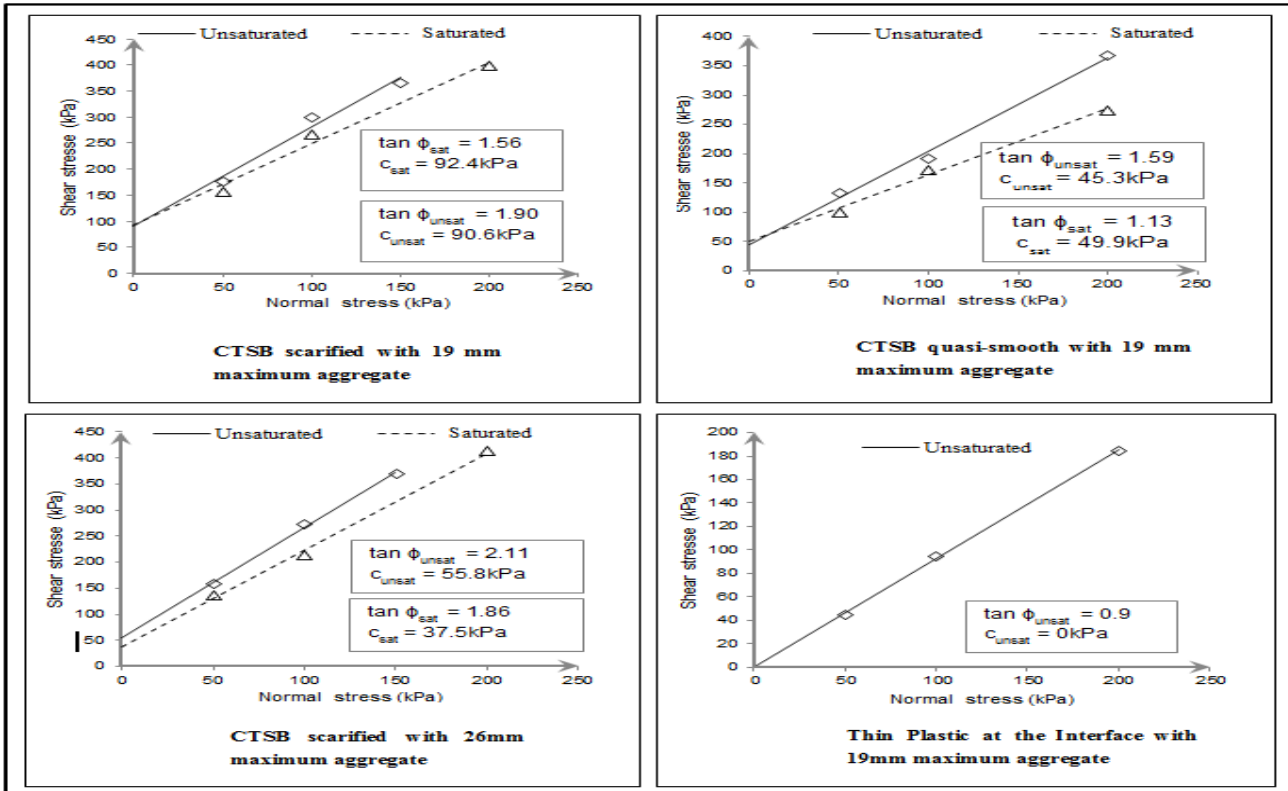


Figure 6: The relationship between shear stress and normal stress for interlayer tests ([25])

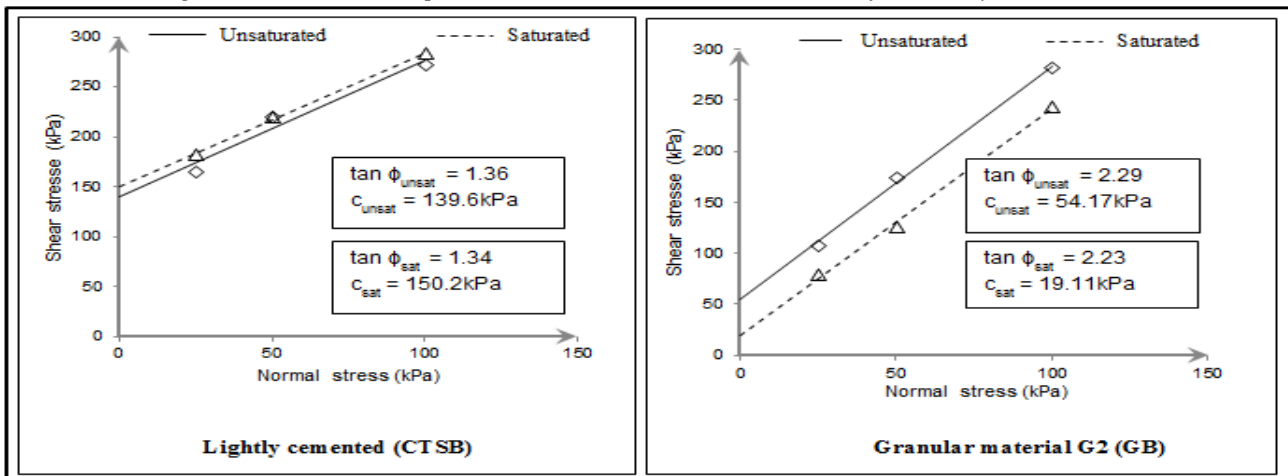


Figure 7: The relationship between shear and normal stresses for intra-layer tests with 19mm aggregate size ([25])

According to the c and μ results presented in Table II, the following observations were made:

- The CTSB surface conditions affected the interlayer friction coefficient. At unsaturated conditions, the value of $\tan \phi$ was reduced from 1.90 when the CTSB was scarified, to 1.59 for the case of quasi-smooth surface. This reduction represents roughly 16%. Moreover, the value of $\tan \phi$ reached 0.93 when the CTSB surface was lined with a thin plastic sheeting before laying the GB. This is equivalent to a 51% reduction. The reduction in friction and cohesion can be explained by lack of intimate contact between layers due to laying the GB on top of hardened and quasi-smooth CTSB.
- A lack of intimate contact between CTSB and GB layers due to a smooth CTSB surface induced high reduction in the interlayer cohesion. A decrease from 90.6 to 45.3kPa was recorded for the unsaturated and 92.4 to 50kPa for the saturated conditions. These correspond to a 50% and 40% reduction respectively.
- An increase in the maximum aggregate size in the CTSB layer from 19 mm to 26 mm caused an increase in the interlayer friction coefficient from 1.90 to 2.11 which correspond to 11%, for the unsaturated condition and 1.56 to 1.86 or 19% for the saturated condition. Moreover, bigger size aggregates induced a reduction in the interlayer cohesion from 90.6kPa to 55.9kPa or 38% reduction for the unsaturated condition and 92.4kPa to 37.5kPa or 59% reduction for the saturated condition. This decrease can be explained by the general behaviour of the granular materials. In fact, the increase in maximum size of aggregate in the mix entailed the decrease of fines ratio and development of a coarse skeleton which had limited contact points. When such a type of mix is compacted and then scarified, the resulting surface seems rougher and coarser compared to that of a material with a small size aggregate. Therefore, laying the GB material on such a surface results in grain to grain contact which leaves open gaps between coarser particles. This therefore leads to an incoherent structure.

According to the relationship between the vertical and horizontal displacement throughout shear testing, the dilation behaviour of samples was evaluated. For each set of testing conditions, the rate of volume change required to mobilise the interlayer shear stress to a critical state was calculated from the respective interlayer shear responses. Maximum values of the dilation rate for the respective normal pressures were used to calculate the angle of dilation in degrees, for each testing condition. In fact, the increase of the dilation angle indicates higher interlocking between layers, thus intimate bondage between them. The resulted average dilation angles are presented in Table III. General trends indicated that the scarified CTSB layer produced higher dilation angles compared to the quasi-smooth surface.

TABLE III: DILATION ANGLE

MAXIMUM SIZE OF AGGREGATE IN CTSB (MM)	CTSB SURFACE CONDITION	SATURATION CONDITION	AVERAGE DILATION ANGLE (Ψ_0)
19	SCARIFIED	UNSATURATED	13.7
		SATURATED	12.1
	QUASI-SMOOTH	UNSATURATED	6.5
		SATURATED	9.1
	WITH PLASTIC	UNSATURATED	4.5
	26	SCARIFIED	UNSATURATED
SATURATED			12.6

From the results shown in Table III, the following was observed:

- The average angle of dilation was reduced by about 12% for the scarified CTSB layer containing 19 mm maximum aggregate size and approximately 15% for 26 mm maximum aggregate size due to the interlayer saturation during shear. This decrease was incited by the lubricant behaviour of the water at the interface between the CTSB and GB layers which softened the particle interlock, therefore resulting in straightaway particle sliding and rearrangement.
- Results of the unsaturated scarified interlayer shear test for 19 mm maximum aggregate in the CTSB offered 13.7° average dilation angle while the one with 26 mm maximum aggregate yields 14.9°. This increase of approximately 9% was induced by the increase in maximum aggregate size in the CTSB.
- The unsaturated non-scarified interlayer shear test for 19 mm aggregate in the CTSB produced 6.5° of average dilation angle while the scarified shear test, with the same aggregate size in the CTSB, produced 13.7°. There was thus an approximate increase of 53% in the dilation angle due to scarification of the CTSB.
- The non-scarified interlayer shear test with 19 mm aggregate size in the CTSB layer produced 6.5° of average dilation angle while the scarified interlayer shear test with 26 mm maximum aggregate size produced 14.9°. This means an increase in average dilation angle by 56% due to the increase in maximum aggregate size in the CTSB and surface scarification.
- The dilation angle can reduce up to 70% when the interaction between the CTSB and the GB is only characterised by simple friction without interlock as simulated by shearing with thin plastic at the interface.

All the above observations shed light on the intimate interaction between scarified CTSB layer and the GB due to particle interlock at the surface contact between the two layers.

B. Comparative Analysis on Interlayer and Intra-layer Shear Performance

In Figure 8, the results of the unsaturated intra-layer and interlayer shear tests are presented whereby the maximum shear stress and the relative horizontal displacement are plotted according to different testing conditions. The comparison was done for 50 and 100kPa normal pressure while the maximum aggregate size in the CTSB for both intra-layer and interlayer tests was limited to 19 mm. Two saturation conditions were considered: saturated and non-saturated. From the intra-layer and interlayer test results shown in Figure 8, the prominent influence of the CTSB layer finishing on the interlayer shear resistance can be observed. By comparing the interlayer and intra-layer shear resistance and the maximum displacement required to fully mobilise the shear stress, it was found that:

- The interlayer shear between the GB and scarified CTSB layer produced the maximum shear stress of 176.6kPa after 16 mm horizontal displacement. This was achieved at 50kPa normal pressure. At 100kPa normal pressure, the maximum shear stress of 299.7kPa was recorded after 15 mm horizontal displacement. For the Intra-layer GB test, the maximum shear stress of 174.2kPa was reached after 20.5 mm horizontal displacement with 50kPa normal pressure. At 100kPa normal pressure, the shear stress at failure turned to 281.9kPa with 19.8 mm horizontal displacement. Comparing the results of intra-layer and interlayer shear tests, it should be concluded that the interlayer shear between the GB and scarified CTSB layer offered approximately equal shear resistance with the intra-layer GB layer at 50kPa normal pressure and slightly higher at 100kPa. However, the horizontal displacement required to fully mobilise the shear stress was lower.
- The interlayer shear resistance between the GB and smooth CTSB was 133.1kPa at 50kPa normal pressure and 191.7kPa at 100kPa normal pressure. Comparing these results with those related to intra-layer GB shear as presented in Figure 7, the decrease of 24% shear resistance for 50kPa normal pressure and 32% for 100kPa should be noticed. The decrease may reach 75% at 50kPa and 67% at 100kPa when the interlock between the GB and CTSB materials was lost as simulated in the worst case scenario.

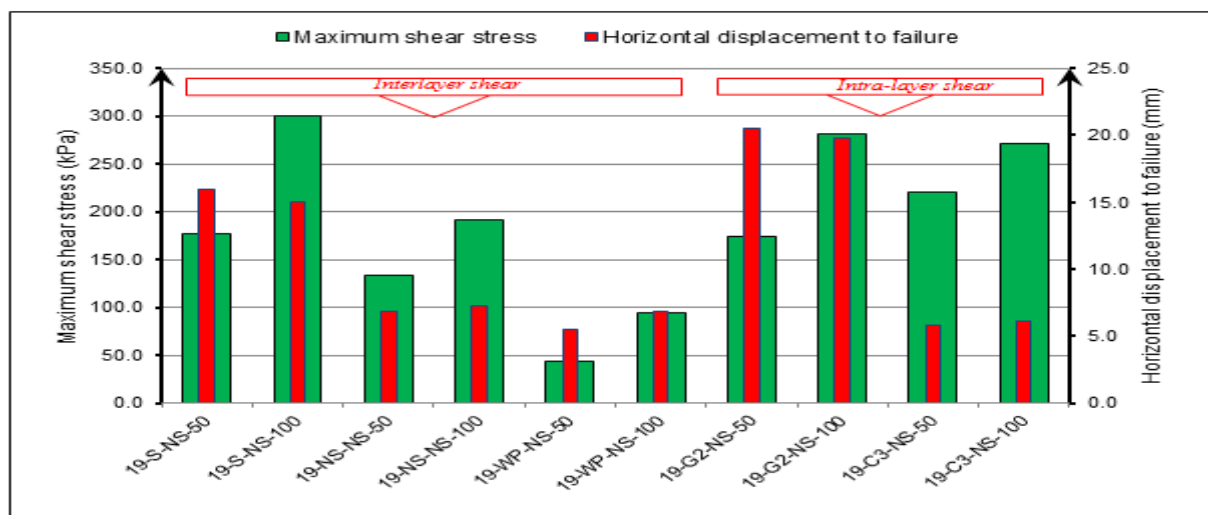


Figure 8: Comparative analysis of intra-layer and interlayer shear stress and relative horizontal displacement to failure for the unsaturated condition ([25]).

The observations above confirmed that the interlayer shear response between GB and CTSB depends on the CTSB surface conditions and applied normal pressure. They also depict that if the CTSB layer is scarified before laying GB, the obtained interlayer shear resistance values are much closer to those attained when the shear plane is located in the middle of the GB layer. Table IV presents the comparison between the interlayer and intra-layer friction coefficients and cohesions for the unsaturated condition. The values presented in Table IV were derived from the shear stress-normal pressure relationships as presented in Figure 9 according to various testing conditions.

The comparative analysis of intra-layer and interlayer response upon shear demonstrated the active influence of the CTSB surface conditions and moisture condition.

From the Mohr-Coulomb failure envelopes plotted in Figure 9, the following observations were made:

- Cohesionless and full slip conditions were noticed for the interlayer shear response with thin plastic sheeting between the GB and CTSB layers as was expected. An interlayer friction coefficient of 0.93 and approximately zero cohesion were observed (see Figure 9).
- The highest friction was observed on the intra-layer shear response of the GB material with friction coefficient of 2.29. The CTSB layer was found to be the most cohesive due to cementation.

TABLE IV: COMPARISON BETWEEN INTERLAYER AND INTRA-LAYER FRICTION COEFFICIENTS AND COHESIONS FOR THE UNSATURATED CONDITION

TYPE OF SHEAR TEST	CTSB SURFACE CONDITION	LABEL	$\mu = \tan \Phi$	Φ (°)	c (kPa)
Interlayer	Scarified	19-S-NS	1.90	62.2	90.6
	Quasi-smooth	19-NS-NS	1.59	57.8	45.3
	With plastic	19-WP-NS	0.93	43	0.7
Intra-layer	Not applicable	19-G2-NS	2.29	66.4	54.2
		19-C3-NS	1.36	53.7	139.6

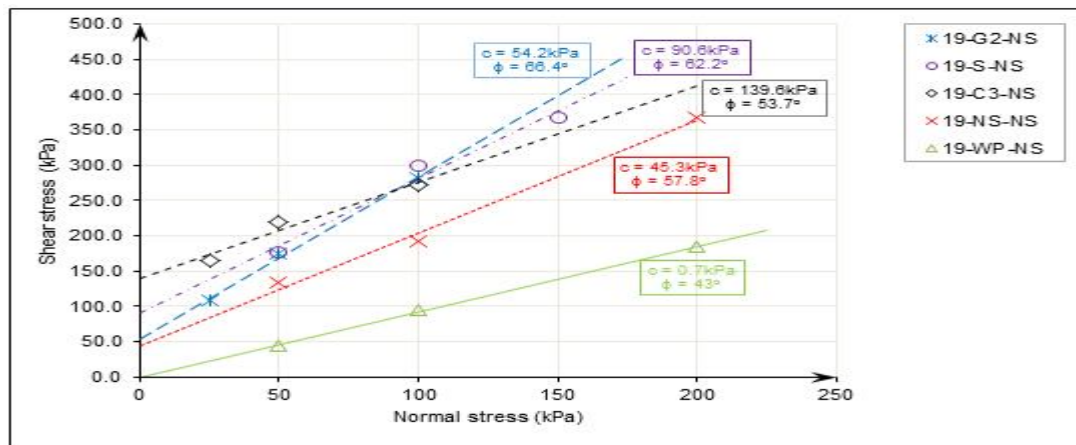


Figure 9: Comparative analysis of intra-layer and interlayer failure envelopes for the unsaturated condition ([25])

- The failure envelope line of interlayer shear response for scarified CTSB and GB interferes with the intersection between the two failure envelope lines of intra-layer GB and CTSB shear and stays between them for a wide range of normal pressure (see Figure 9). Therefore, according to the observation presented in the previous paragraph, the failure envelope path of the scarified CTSB and GB structure seems to confirm that scarifying the CTSB layer before laying the GB provides the most efficient conditions in both cohesion and friction.
- The failure envelope of the interlayer shear between quasi-smooth CTSB and GB remains between two failures envelopes of extreme conditions defined above. This implicated the reduction of interlayer friction coefficient by 30% compared to the highest friction conditions observed.

All the observations above supported the influence of CTSB surface scarification on the interlayer friction and cohesion behaviour between the GB and CTSB layers.

In Figure 10, the average dilation angles are presented for the intra-layer and interlayer shear tests.

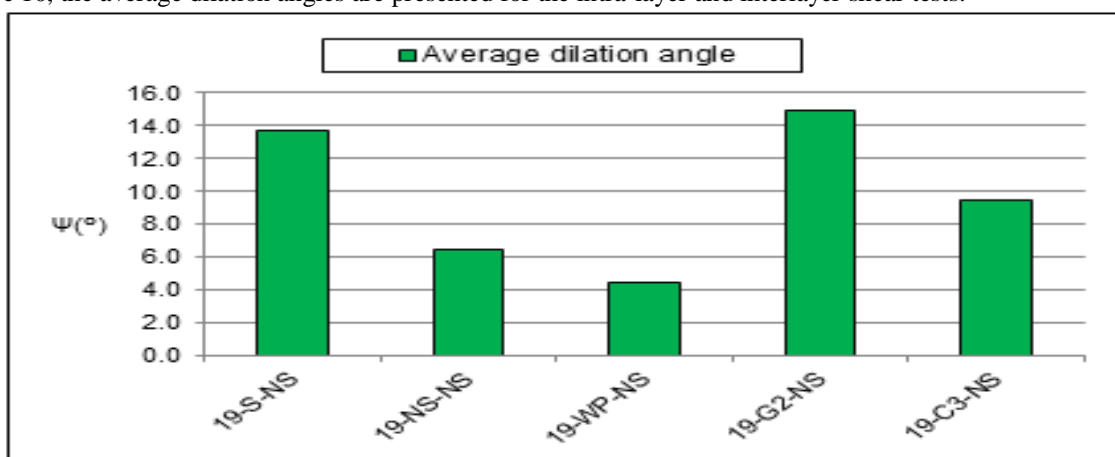


Figure 10: Comparative analysis of dilation between intra-layer and interlayer shear test for the unsaturated condition. The comparative analysis of dilation angles related to the interlayer and intra-layer shear tests (Figure 10) highlighted the influence of the CTSB surface roughness on its interaction with the GB layer. From Figure 10, the following were observed:

- For the interlayer shear test, the value of the highest dilation angle was 13.7° which was achieved when the surface of the CTSB layer was scarified before laying the GB. This value was fairly close to the dilation angle obtained from the intra-layer shear test of the GB layer which was 14.9° .
- The value of the dilation angle corresponding to the interlayer shear test between quasi-smooth CTSB and GB was 6.5° . When it is compared to the intra-layer response of the GB, which has a 14.9° dilation angle, the smooth CTSB-GB structure reveals a reduction of dilation by up to roughly 56%. When the comparison is done between intra-layer GB ($\Psi=14.9^\circ$) and interlayer shear with plastic between the CTSB and GB ($\Psi=4.5^\circ$), a reduction of the dilation angle by up to 70% can be observed.

The dilation angles obtained from various testing conditions revealed the correlation between dilation behaviour and the adherence of the GB to the CTSB. Scarification of the CTSB exhibited a greater dilation angle which was closer to the value obtained for the GB intra-layer shear test. Therefore, it should be concluded that when the surface of the CTSB layer is scarified before laying the GB layer, the yield interlayer shear resistance is much closer to the resistance in the middle of the GB layer.

IV. PRACTICAL SIGNIFICANCE

A typical pavement design example was conducted to illustrate the practical influence of the frictional interaction between layers on the overall pavement performance. The structural design considered a Category A road in the South African road categories ([19]). The design principle, however, can equally be adopted for all other road categories. The analysis of stress-strain distribution throughout the pavement structure was carried out with BISAR software for various interlayer friction conditions. Finally, the total number of load repetitions that every layer can sustain before reaching specific terminal conditions was computed for each interlayer friction parameter. The computation was based on the material failure mode and relevant critical parameters as specified in the South African Mechanistic Design Method (SAMDM). Using the results of this study, an attempt was made to develop a correlation chart between the interlayer adhesion ratio computed from the laboratory tests and the interlayer friction parameter (α) which is used in BISAR software analysis.

A. Typical Structural Design and Pavement Life Estimation

Normally the SAMDM assumes full friction between layers. However, this does not represent the real conditions in the field ([16], [11] and [23]). The use of BISAR software allowed the modelling of the pavement structure with different interlayer friction conditions which were defined by the parameter - α (i.e. $\alpha = 0$ means full friction and $\alpha = 1$ means full slip). For the purpose of this analysis, a range of interlayer friction parameters was selected and then correlated to the actual conditions considered in this study. The selection of interlayer friction parameters was done in such a way that a sufficient range of partial friction between the GB and the CTSB layers was covered. The pavement structure considered in this design example is for the interurban road characterised by a high volume of traffic, and many heavy vehicles. The design traffic loading for this category ranges between 3 and 10×10^6 standard axles (80kN axles/lane) over 20 years with the approximate design reliability of 95% ([19]). The analysis used the loading configuration comprising an 80kN axle with one super single tyre at each end and the tyre pressure was kept at 750kPa ([18], [13] and [12]).

Table V shows the mechanical properties of materials used to model the pavement layers. Properties were selected according to SAPEM's recommendations.

TABLE V: MECHANICAL PROPERTIES OF MATERIALS USED TO MODEL PAVEMENT LAYERS

LAYER	TYPE OF MATERIAL MODELLING	THICKNESS (MM)	E (MPA)	ν (-)
ASPHALT	LINEAR ELASTIC	40	2500	0.35
GRANULAR BASE G2	NON-LINEAR ELASTIC	150	400	0.45
CEMENTED SUBBASE C3	LINEAR ELASTIC	250	1500	0.4
SUBGRADE G10	LINEAR ELASTIC	INFINITE	50	0.4

According to the predefined interlayer friction conditions, reduced spring compliances have been computed and introduced to BISAR software with other input parameters for the analysis. Figure 11 and Figure 12 illustrate stress and strain distribution throughout the pavement structure when various friction conditions are considered. Note that α_1 and α_2 stand for interlayer friction parameters for AC/GB and GB/CTSB interlayers respectively. For all modelling cases, full bond was assumed between the CTSB and sub grade (SG) layers. In Figure 11, curves of vertical and horizontal strain distribution across the pavement structure are shown. It can be seen that higher vertical strain is developed across the granular base and on top of the subgrade as interlayer friction diminishes. This behaviour has a direct influence on the permanent deformation of the layer and subsequently the deformation of the road surface. From the horizontal strain distribution curve it can be observed that the increase of tensile strain at the bottom or within the asphalt layer as friction between the layers diminishes. This indicates its influence on the structure's load spread behaviour. The direct effect of more strain in the AC layer is the speeding up of the development of fatigue cracks at the bottom or within the layer.

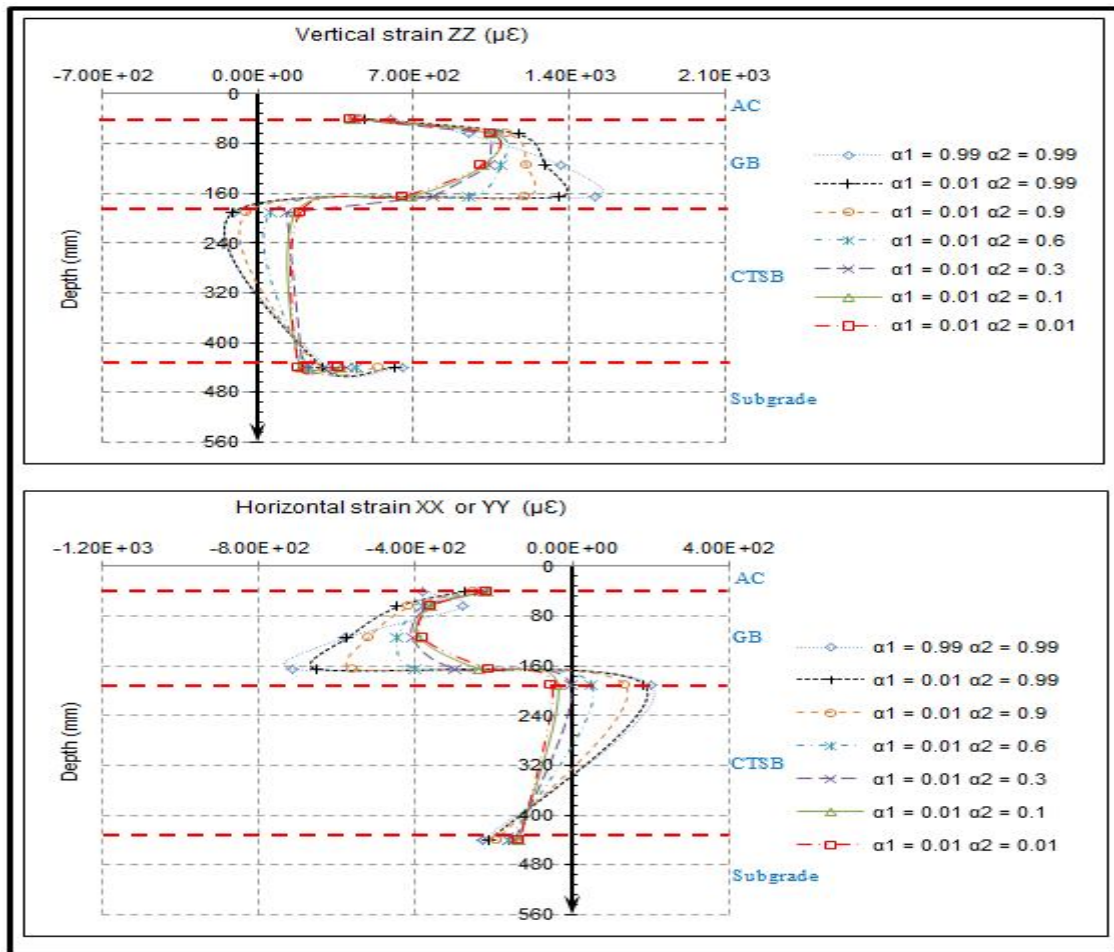


Figure 11: Vertical and horizontal strain distribution curve across the pavement structure with variation in interlayer friction ([25])

In addition, Figure 11 shows a rapid increase in horizontal tensile strain in the granular base as full friction between the GB and CTSB diminishes. This justifies the significant reduction in the layer's life (see Figure 14) since granular materials are weak in tension. Figure 12 presents the vertical and horizontal stress distribution curves. The load spreading response of the pavement structure from the top to the subgrade can be observed in the vertical stress distribution curve, but the influence of the interlayer friction conditions is not well established. On the other hand, the horizontal stress distribution curves, also shown in Figure 12 presents a marked increase in horizontal stress at the GB/CTSB interface as interlayer friction diminishes. This reaction might induce significant shear flow between layers and subsequently, interface shear failure. From the stress-strain distribution analysis, it can be concluded that the interlayer friction conditions between the GB and the CTSB has a significant influence on material response in the pavement structure. The granular base layer was observed to become more sensitive to traffic induced loading as the interlayer friction parameter changes from full friction ($\alpha = 0$) towards full slip ($\alpha = 1$). This sensitivity was attributed to the stress-dependency behaviour of granular materials. In the SAMDM, the total number of load repetitions that a pavement can withstand before reaching terminal conditions is estimated according to stress and strain values at a particular position in each layer which is termed as the critical position. Every layer exhibits a specific mode of failure and particular mathematical models are used to estimate the associated life of each layer. In Figure 13 the estimated life of the hot mix asphalt layer is plotted against the interlayer friction parameters. The general trend shows that the life of the layer is sensitive to the interlayer adhesion conditions. The number of load repetitions reduces as friction between the GB and CTSB diminishes. For instance, by assuming full friction between the AC and GB layers ($\alpha_1 = 0.01$), the change of friction conditions between the GB and CTSB from full friction ($\alpha_2 = 0.01$) to partial friction ($\alpha_2 = 0.6$) induces the reduction of the load repetitions from $2.79E+05$ to $1.90E+05$. This means an approximate 32% reduction in the layer's life. The general observation from the analysis is that the capacity of the asphalt layer to sustain traffic induced loading is affected by the interlayer friction conditions between the GB and CTSB layers. To estimate the life of the base layer, the SAMDM approach was used whereby the failure is assumed to take place in the middle of the layer. The transfer function for a Category A road was used to calculate the total number of load repetitions that the layer could withstand before its failure and values were presented in Figure 14 against the interlayer friction parameters.

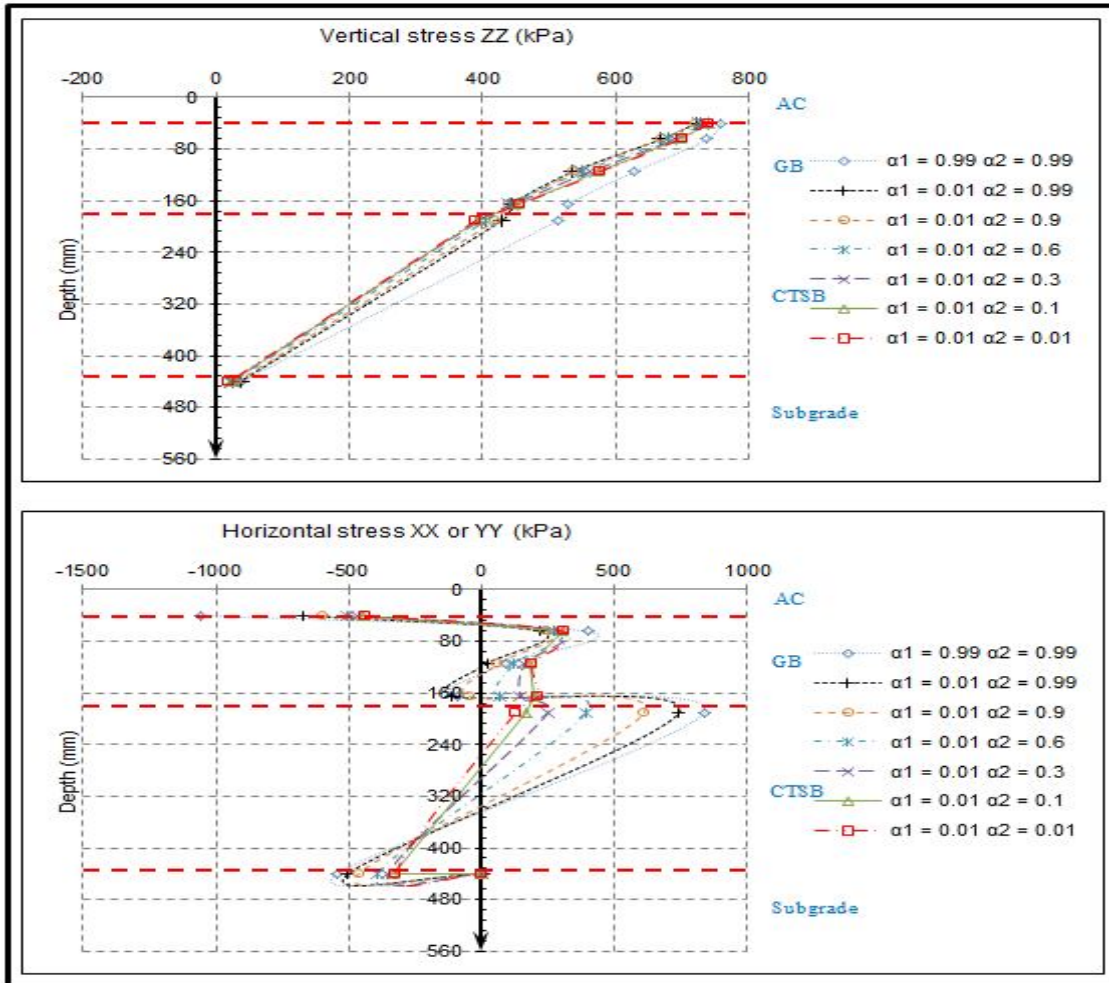


Figure 12: Vertical and horizontal stress distribution across the pavement structure with variation in interlayer friction ([25])

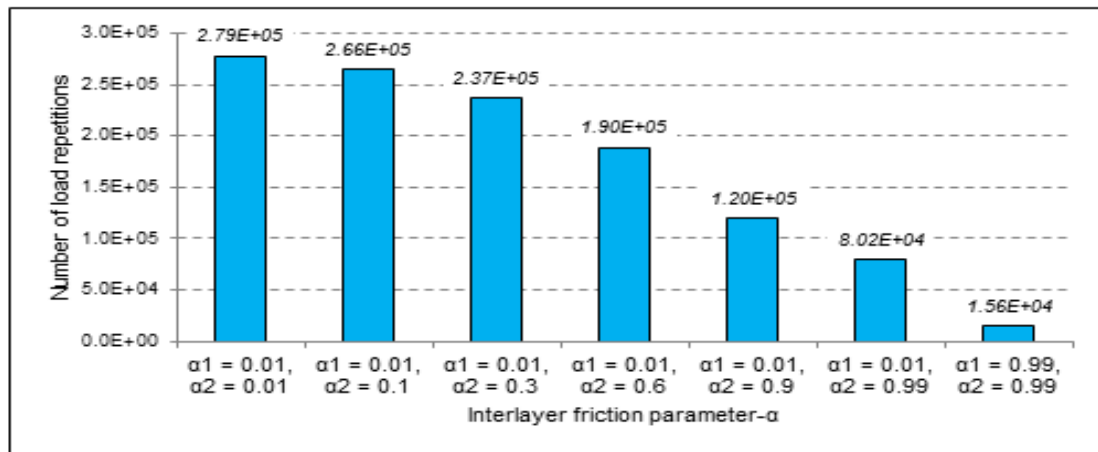


Figure 13: The influence of interlayer friction conditions on the life of the asphalt layer

The graph presented in Figure 14 highlights the typical response of the granular base when a slight reduction in interlayer friction is allowed in the vicinity of the ideal zone. This reduction of the interlayer friction results in a quick drop of a layer's life. The magnified perspective can be used to explain the behaviour of the GB when interlayer friction reduces. In fact, when the GB layer is placed on top of the CTSB in such a way that maximum adhesion is achieved, the two layers act in unison and the new equivalent layer thickness yield a significant load carrying capacity as can be visualised in Figure 14 for $\alpha_2 = 0.1$. However, if slight slip between the two layers is allowed to occur, immediate release of particles will take place due to unbound behaviour of the granular materials. Therefore the kneading action of the tyre on the pavement surface will induce granular particles to scramble and give way to the CTSB to endure the load.

This reaction will quickly deteriorate the base layer as can be noticed in Figure 14 whereby the life of the layer was reduced considerably from 1.4E+12 to 1.2E+11 when the interlayer friction parameter was only changed from 0.1 to 0.3.

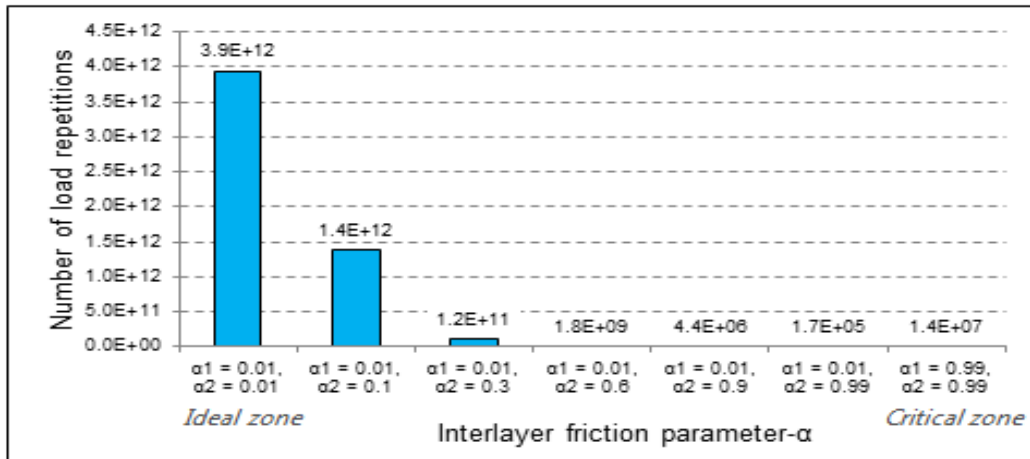


Figure 14: The influence of interlayer friction conditions on the life of the granular base layer

From the above observations, it can be concluded that the structural performance of a GB layer is highly sensitive to the achievable interlayer adhesion conditions. A slight reduction in interlayer friction causes a significant reduction in the load carrying capacity of the layer. Lives of the CTSB and the subgrade are plotted against the interlayer friction parameters and presented in Figure 15 and Figure 16 respectively. The general observation from Figure 15 is that both the tensile strain in the CTSB layer and vertical compressive stress on top of the layer increase as the interlayer friction diminishes. This behaviour comes from poor interaction between layers which obstruct smooth distribution of stresses throughout the entire structure. It should also be noted from Figure 16 that the loss of full adhesion between the GB and CTSB layers induced early development of surface ruts due to the deformation of the subgrade material.

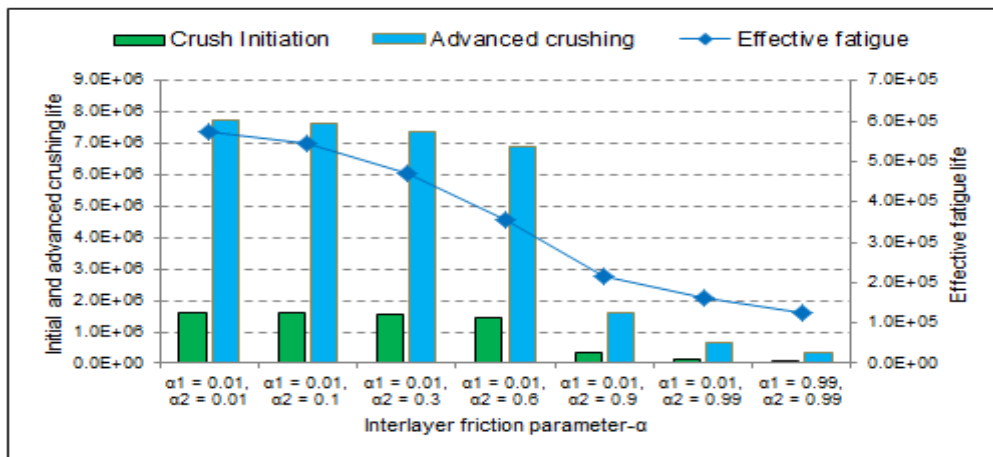


Figure 15: The influence of interlayer friction conditions on the performance of the CTSB layer

Based on the results of change in life to failure for all layers, it can be concluded that the influence of poor adhesion between the GB and the CTSB on the pavement performance was noticeable upon each layer of the pavement structure. The life of every layer showed a substantial decrease when partial friction was allowed. The GB showed early failure compared to other layers.

B. Correlation between Achievable Adhesion and Pavement Life

According to the routine construction technique followed in the field, the GB layer is compacted on top of the non-scarified CTSB layer. In the current study, this condition was simulated by shearing the interface between GB and quasi-smooth CTSB. The correlation between the achievable adhesion and the interlayer friction parameter used in BISAR software shows that the interlayer friction conditions of the GB and quasi-smooth CTSB corresponds to α parameter ranging between 0.5 and 0.7, while for the GB and scarified CTSB it is closer to 0.1. Figure 17 presents the associated number of axle loads for scarified and quasi-smooth CTSB. The total number of standard axles to failure are simulated by $\alpha = 0.1$ for the scarified CTSB and the average between 0.5 and 0.7 or $\alpha = 0.6$ for the quasi-smooth CTSB. From the results of the correlation between the achievable adhesion and the interlayer friction parameter as presented in Figure 17, it is apparent that the interlayer adhesion strength between the GB and the CTSB significantly influences the performance of each individual layer in the pavement structure.

The total number of standard axles that every layer can withstand before failure reduces considerably when the GB is laid on top of non-scarified CTSB. For this design example, the GB layer was found to be most affected by the adhesion conditions.

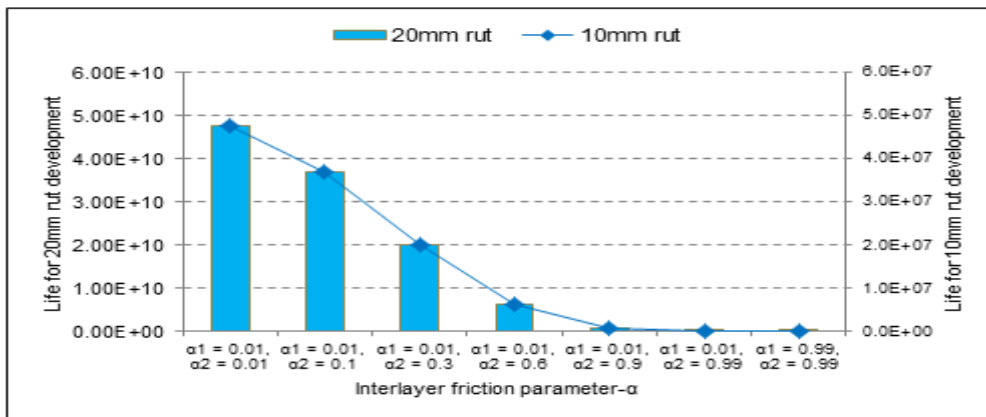


Figure 16: Life of the subgrade layer according to different interlayer friction conditions

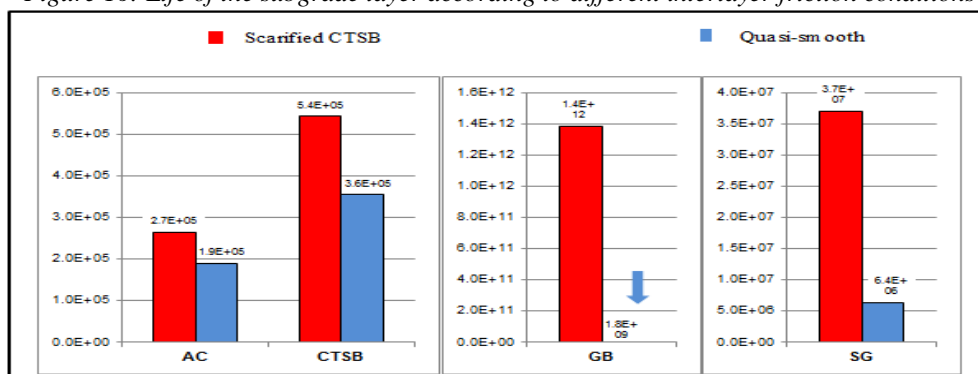


Figure 17: Comparison of total number of load repetitions to failure for scarified and quasi-smooth CTSB

V. CONCLUSIONS AND RECOMMENDATIONS

The main purpose of this study was to investigate the achievable interlayer adhesion strength between the GB and the CTSB layers and assess its influence on the general performance of the pavement structure. Laboratory testing and theoretical analysis approaches were followed to achieve the study objectives. A typical structural design served as a basis to acquire understanding of the influence of interlayer adhesion on the pavement performance, especially for the routine construction technique used in the field.

Considering the results of this study the following conclusions and recommendations can be made:

1. Practically the staged construction procedure of the CTSB and GB involves laying base materials on a previously hardened CTSB layer. This prohibits the unification of the two layers. However, scarifying the CTSB top surface before curing the layer and laying the GB improves the intimate contact between the two layers and results in unison interaction and marked improvement in pavement life.
2. Scarifying the top surface of the CTSB before curing the layer and laying the GB offers the interlayer shear strength which is nearly equal to the intra-layer shear strength across the GB layer. This thus confirms high interlayer adhesion due to scarification.
3. Correlation of the achievable adhesion between the GB and CTSB with the interlayer friction parameter showed that the routine construction process followed in the field induces a significant reduction in the number of standard axle loads that a layer can withstand before reaching specific failure conditions.
4. Considering the influence of scarification on the improvement of interlayer shear strength between the GB and the CTSB, it is recommended that this practice be incorporated in the routine construction practice. In order to avoid carbonation of loose materials left after scarification of the CTSB, it is recommended to sweep the surface before laying the GB.
5. Presently, the influence of poor interlayer adhesion on the pavement performance is becoming critical. However, substantial knowledge about the interaction between layers and related failure mechanism is still lacking. It is therefore recommended to mobilise different research to deepen the understanding of the subject and to develop coherent and scientifically based views. This will give rise to technical specifications and guidelines to be followed for achieving proper shear interaction in the field.

REFERENCES

- [1]. Canestrari, F., Ferrotti, G., Partl, M.N. & Santagata, E. 2005. *Advanced Testing and Characterization of Interlayer Shear Resistance*. Transportation Research Record: Journal of the Transportation Research Board, 1929(1).
- [2]. Canestrari, F. & Santagata, E. 2005. *Temperature Effects on the Shear Behaviour of Tack Coat Emulsions used in Flexible Pavements*. International Journal of Pavement Engineering, 6(1): 39-46.
- [3]. Choi, Y., Sutanto, M., Collop, A. & Airey, G. 2006. *Bond between Asphalt Layers*. Project Report to the UK Highways Agency, Scott Wilson Pavement Engineering Ltd., Nottingham, UK.
- [4]. D'Andrea, A. & Tozzo, C. 2012. *Interlayer Shear Failure Evolution with Different Test Equipments*. Procedia-Social and Behavioral Sciences, 53
- [5]. D'Andrea, A., Tozzo, C., Boschetto, A. & Bottini, L. 2013. *Interface Roughness Parameters and Shear Strength*. Modern Applied Science, 7(10).
- [6]. Edwards, J.P. 2007. *Laboratory characterisation of pavement foundation materials*. Doctoral dissertation. Loughborough: Loughborough University.
- [7]. Geocomp. 2012. *Shear Trac III system, Load frame system for Running Fully Automated Direct and Interface Shear Tests on Soil and Geosynthetics using Windows XP/Vista/7*. User's Manual. Geocomp Corporation. USA
- [8]. Hariyadi, E.S., Aurum, K.P. and Subagio, B.S. 2013. *Theoretical Study of Bonding Condition at the Interface between Asphalt Pavement Layers*. Paper presented at Proceedings of the Eastern Asia Society for Transportation Studies.
- [9]. Jenkins, J.K. 2013. *Hitchhiker's guide to pavement engineering*. Pavement material I unpublished lecture notes. Stellenbosch: Stellenbosch University.
- [10]. Jooste, F. 2004. *A Re-Evaluation of Some Aspects of the Mechanistic-Empirical Design Approach*. Paper presented at Proceedings of the 8th Conference on Asphalt Pavements for Southern Africa (CAPSA'04).
- [11]. Kruntcheva, M.R., Collop, A.C. & Thom, N.H. 2005. *Effect of Bond Condition on Flexible Pavement Performance*. Journal of Transportation Engineering, 131(11): 880-888.
- [12]. Molenaar, A. 2007. *Design of Flexible Pavement*, Lecture Note CT 4860 Structural Pavement Design. Delft: Delft University of Technology.
- [13]. Morton, B.S., Luttig, E., Horak, E. and Visser, A. 2004. *The Effect of Axle Load Spectra and Tyre Inflation Pressures on Standard Pavement Design Methods*. Paper presented at 8th Conference of Asphalt Pavements of Southern Africa (CAPSA).
- [14]. Raab, C., Partl, M.N. & El Halim, O.A. 2009. *Evaluation of Interlayer Shear Bond Devices for Asphalt Pavements*. Baltic Journal of Road and Bridge Engineering, 4(4): 186-195.
- [15]. SAPEM. 2013. *South African Pavement Engineering Manual 1st edition*. South African National Roads Agency Ltd, Pretoria, Republic of South Africa.
- [16]. Sutanto, M., Collop, A., Airey, G., Elliott, R. and Choi, Y. 2006. *Laboratory Measurement of Bond between Asphalt Layers*. Paper presented at Proceedings of the 5th International Conference on Research and Practical Applications Using Wastes and Secondary Materials in Pavement Engineering Held 22-23 February 2006, Liverpool, UK-Vol 1-Day One, Vol 2-Day Two.
- [17]. Theyse, H., De Beer, M., Maina, J. & Kannemeyer, L. 2011. *Interim Revision of the South African Mechanistic-Empirical Pavement Design Method for Flexible Pavements*.
- [18]. Theyse, H. and Muthen, M. 2000. *Pavement Analysis and Design Software (PADS) Based on the South African Mechanistic-Empirical Design Method*. Paper presented at South African Transport Conference (SATC). Action in Transport for the new Millennium.
- [19]. TRH4. 1996. *Structural design of flexible pavements for interurban and rural roads*. Pretoria, South Africa: Department of Transport
- [20]. TRH14. 1985. *Guidelines for road construction materials*. Pretoria, South Africa: Department of Transport
- [21]. Uzan, J. 1976. *Influence of the interface condition on stress distribution in a layered system (abridgement)*. Transportation Research Record, (616): 71-73.
- [22]. Uzan, J., Livneh, M. and Eshed, Y. 1978. *Investigation of Adhesion Properties between Asphaltic-Concrete Layers*. Paper presented at Association of Asphalt Paving Technologists Proc.
- [23]. Whiffin, A. and Lister, N. 1962. *The Application of Elastic Theory to Flexible Pavements*. Paper presented at International Conference on the Structural Design of Asphalt Pavements.
- [24]. Ziari, H. & Khabiri, M.M. 2007. *Interface Condition Influence on Prediction of Flexible Pavement Life*. Journal of Civil Engineering and Management, 13(1): 71-76.
- [25]. Ntiringanya, N. 2015. *An Investigation of the Interlayer Adhesion Strength between the Granular Base and Lightly Cemented Subbase and Its Influence on the Pavement Performance*, Masters thesis. Stellenbosch: University of Stellenbosch.